Food Research International 137 (2020) 109539

Contents lists available at ScienceDirect

Food Research International

journal homepage: www.elsevier.com/locate/foodres

Slow lactate gluconate exchange in calcium complexes during precipitation from supersaturated aqueous solutions

André C. Garcia[a,b], Jesper S. Hansen[c], Nicholas Bailey[c], Leif H. Skibsted[a,*]

[a] Department of Food Science, University of Copenhagen, Rolighedsvej 30, DK-1958 Frederiksberg C, Denmark
[b] Instituto Federal de Educação, Ciência e Tecnologia de São Paulo, Campus Capivari. Avenida Doutor Ênio Pires de Camargo, 2971, São João Batista, CEP: 13360-000 Capivari, SP, Brazil
[c] IMFUFA, Department of Science and Environment, Roskilde University, Universitetsvej 1, DK-4000 Roskilde, Denmark

ARTICLE INFO

Keywords:
Supersaturation
Calcium hydroxycarboxylates
Kinetic modelling

ABSTRACT

Saturated solutions of calcium L-lactate in water or in deuterium oxide continuously dissolve calcium L-lactate by addition of solid sodium D-gluconate and become strongly supersaturated in calcium D-gluconate due to no or slow precipitation. The quantification of total dissolved calcium allied with the calcium complexes equilibrium constants allowed an ion speciation, which shows an initial non-thermal and spontaneous supersaturation of more than a factor of 50 at 25 °C only slowly decreasing after initiation of precipitation of calcium D-gluconate after a lag phase of several hours. A mathematical model is proposed, based on numerical solution of coupled differential equations of dynamics of L-lactate and D-gluconate exchange during the lag phase for precipitation and during precipitation. A slow exchange of L-lactate coordinated to calcium with D-gluconate is indicated with a time constant of 0.20 h^{-1} in water and of 0.15 h^{-1} in deuterium oxide and a kinetic deuterium/hydrogen isotope effect of 1.25. Such spontaneous non-thermal supersaturation and slow ligand exchange with a pseudo first order equilibration process with a half-life of 3.5 h in water for calcium hydroxycarboxylates can help to understand the higher calcium bioavailability from calcium hydroxycarboxylates compared to simple salts.

1. Introduction

Calcium salts of hydroxycarboxylic acids, like L-lactic acid, D-gluconic acid and citric acid are known to be better dietary supplements with higher calcium bioavailability compared to calcium carbonate and other inorganic calcium salts for better bone health and for prevention of osteoporosis (Adluri, Zhan, Bagchi, Maulik, & Maulik, 2010; Pak, Harvey, & Hsu, 1987; Tondapu et al., 2009). The transfer of the chyme from the acidic digestion in the stomach to the increasing pH environment of the intestines, where most of the calcium absorption occurs, carries the risk of initiating precipitation of calcium phosphates, calcium carbonate and calcium phytate, leading to calcium malabsorption even from a diet rich in calcium (de Boland, Garner, & O'Dell, 1975; Wasserman, 2004).

Calcium absorption in the intestines occurs by a trans-cellular mechanism depending on vitamin D, and by a para-cellular vitamin D independent diffusion mechanism of calcium ions. For both mechanisms soluble calcium is important and the higher bioavailability of calcium from hydroxycarboxylates than from more simple calcium salts may be the result of complex binding of calcium preventing precipitation (de Barboza, Guizzardi, & de Talamoni, 2015). Supersaturation of calcium hydroxycarboxylates in the intestines may, however, be of even higher importance for sufficient calcium bioavailability explaining the superiority of calcium hydroxycarboxylates as calcium supplements. The recent demonstration a positive correlation between high circulating citrate and bone strength further points toward the importance of hydroxycarboxylates for calcium resorption and mineralization (Hartley et al., 2019; Wang et al., 2012).

Calcium hydroxycarboxylates have been shown to form spontaneous and robust supersaturated aqueous solutions by non-thermal dissolution of solid calcium salts in excess of ionic hydroxycarboxylates (Vavrusova & Skibsted, 2014; Vavrusova, Garcia, Danielsen, & Skibsted, 2017). The lag phase for initiation of precipitation from such highly supersaturated solutions depends on the nature and the concentration of the hydroxycarboxylates. For specific combinations and conditions, lag phases of several months have been observed (Siegrist, 1949; Vavrusova, Liang, & Skibsted, 2014).

The dynamics behind spontaneous supersaturation upon dissolution of calcium hydroxycarboxylates in water are largely unknown as are the kinetics of precipitation from such often highly supersaturated

* Corresponding author.
E-mail address: ls@food.ku.dk (L.H. Skibsted).

https://doi.org/10.1016/j.foodres.2020.109539
Received 25 May 2020; Received in revised form 22 June 2020; Accepted 9 July 2020
Available online 15 July 2020

solutions. For the combination of calcium L-lactate and sodium D-gluconate, the spontaneous supersaturation is instantaneous and substantial and we have selected this combination for a study of the dynamics behind the robustness of the supersaturation and the kinetics of precipitation. An experimental study is combined with mathematically modeling in order to obtain results of more general validity for calcium turnover during biological mineralization (Holt, Lenton, Nylander, Sørensen, & Teixeira, 2014).

2. Material and methods

2.1. Chemicals

Calcium L-lactate pentahydrate, sodium D-gluconate and deuterium oxide were from Sigma-Aldrich (Steinheim, Germany). All reagents were of analytical grade, and the aqueous solutions were made from purified water from Milli-Q Plus (Millipore Corporation, Bedford, MA, USA).

2.2. Samples

All the investigated samples were prepared by adding 3.0 g of calcium L-lactate in 20 mL of water or D_2O, which were kept at 25.0 °C under constant stirring for 2 h. After equilibration, sodium D-gluconate was added in different amounts: 10.4 g, 15.6 g and the intermediate amount of 13.0 g in D_2O. The samples were kept at 25.0 °C under constant stirring, from which aliquots of 100 μL were periodically collected and analysed for total dissolved calcium. All samples were prepared in duplicate.

2.3. Total calcium determination

The aliquots of the samples were filtered through a 0.22 μm cellulose acetate syringe filter (Q-Max RR, Knebel, Denmark), from which 10 μL was added to 9.99 mL of nitric acid 5% using micropipettes from Thermo Scientific (Espoo, Finland). Total calcium was quantified in the samples using an Agilent 5100 inductively coupled plasma – optical emission spectrometer, ICP-OES, (Santa Clara, CA, USA) monitoring the wavelength of 422.673 nm.

3. Results and discussion

Prior to the analyses, the volumes of the samples were measured after the addition of calcium L-lactate and sodium D-gluconate; Table 1 presents the samples compositions and their volumes.

A couple of minutes after the addition of sodium D-gluconate to the saturated solutions of calcium L-lactate, the excess of calcium L-lactate dissolved completely resulting in a clear solution, from which calcium D-gluconate precipitated slowly after a log phase of several hours, as previously described (Vavrusova & Skibsted, 2014). Total calcium concentration was quantified periodically in the three samples. Fig. 1 presents the total calcium concentration from the two duplicates up to 50 h for samples A and B and 72 h for sample C.

In order to better comprehend the thermodynamics and kinetics behind the supersaturation, the ion speciation of the samples was calculated from the results of the determination of the total calcium

Table 1
Samples' compositions and total volumes after the addition of the salts. The sample prepared with deuterium oxide is represented with a subscript "d".

Sample	Calcium L-lactate, g	Sodium D-gluconate, g	Total volume, mL
A	3.0	10.4	26.0
B	3.0	15.6	29.0
C_d	3.0	13.0	28.0

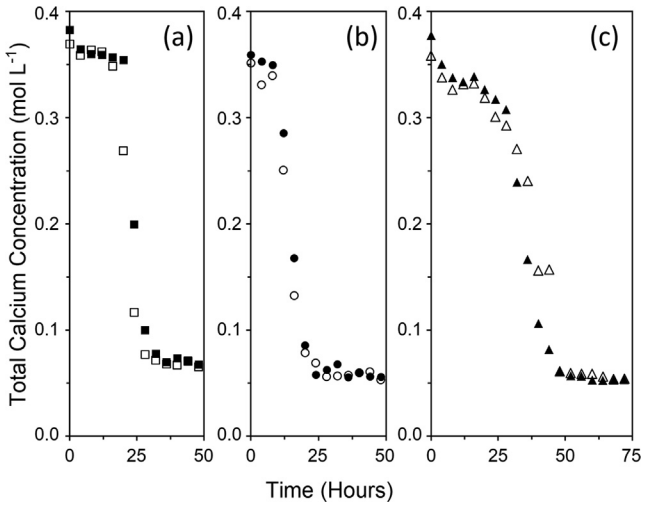

Fig. 1. Total calcium concentration as a function of time, solid and hollow points represent different sets of results for each duplicate of the samples.

concentration and based on the following chemical equilibrium equations and mass balances, assuming equilibrium:

$$Ca^{2+} + Lac^{-} \rightleftharpoons CaLac^{+} \quad (1)$$

$$K_1 = \frac{[CaLac^{+}]}{[Ca^{2+}][Lac^{-}]} \quad (2)$$

$$Ca^{2+} + Glu^{-} \rightleftharpoons CaGlu^{+} \quad (3)$$

$$K_2 = \frac{[CaGlu^{+}]}{[Ca^{2+}][Glu^{-}]} \quad (4)$$

$$t_{Ca^{2+}} = [Ca^{2+}] + [CaLac^{+}] + [CaGlu^{+}] \quad (5)$$

$$t_{Lac^{-}} = [CaLac^{+}] + [Lac^{+}] \quad (6)$$

$$t_{Glu^{-}} = [CaGlu^{+}] + [Glu^{+}] \quad (7)$$

where $t_{Ca^{2+}}$, $t_{Lac^{-}}$, and $t_{Glu^{-}}$ represent total concentrations of calcium, L-lactate and D-gluconate, respectively.

The association constants K_1 and K_2 at 25 °C for high ionic strength are equal to 8 mol^{-1} L and 14 mol^{-1} L, respectively (Vavrusova, Munk, & Skibsted, 2013). It was assumed that all L-lactate remained in solution and that the precipitate was calcium D-gluconate, as previously characterized for this system (Vavrusova & Skibsted, 2014). The calculations of the ion speciation depended on solving the five equations to yield five unknown concentrations: $[Ca^{2+}]$, $[CaLac^{+}]$, $[CaGlu^{+}]$, $[Lac^{-}]$, and $[Glu^{-}]$. Tables 2–4 present the results of the ion speciation for samples A, B and C_d, respectively.

To verify the supersaturation of the samples, Tables 2–4 present ratios of the ionic product, Q, to solubility product, K_{sp}, for calcium L-lactate, $Q_L = [Ca^{2+}][Lac^{-}]^2$, and for calcium D-gluconate, $Q_G = [Ca^{2+}][Glu^{-}]^2$. The solubility products for calcium L-lactate and calcium D-gluconate at high ionic strength are equal to $K_{sp_L} = 5.8 \cdot 10^{-3}$ mol^3 L^{-3} and $K_{sp_G} = 7.1 \cdot 10^{-4}$ mol^3 L^{-3}, respectively (Vavrusova et al., 2013).

As previously reported (Garcia et al., 2016, 2018; Vavrusova & Skibsted, 2014; Vavrusova et al., 2017, 2018), this spontaneous supersaturation phenomenon occur due to a combination of thermodynamic and kinetic effects: stronger complex formation between calcium and D-gluconate ions and slow precipitation rate of calcium D-gluconate. In order to better comprehend the precipitation kinetics, a mathematical model is proposed based on the dynamics of the calcium L-lactate and calcium D-gluconate complexes, $CaLac^{+}$ and $CaGlu^{+}$, as well as on the calcium D-gluconate precipitation and dissolution. From the ion speciation calculations, it was verified that free calcium concentration, $[Ca^{2+}]$, was always smaller than 5% of total calcium

Table 2
Ion speciation for sample A, concentrations expressed in mol L^{-1} and time expressed in hours. Total L-lactate concentration, t_{Lac^-}, equal to $7.49 \cdot 10^{-1}$ mol L^{-1}.

Time	t_{Glu^-}	$[CaLac^+]$	$[Ca^{2+}]$	$[Lac^-]$	$[CaGlu^+]$	$[Glu^-]$	Q_L/K_{sp_L}	Q_G/K_{sp_G}
0.02	1.83	$7.26 \cdot 10^{-2}$	$1.34 \cdot 10^{-2}$	$6.76 \cdot 10^{-1}$	$2.90 \cdot 10^{-1}$	1.54	1.06	45.0
4	1.81	$7.06 \cdot 10^{-2}$	$1.30 \cdot 10^{-2}$	$6.78 \cdot 10^{-1}$	$2.78 \cdot 10^{-1}$	1.53	1.03	42.7
8	1.81	$7.06 \cdot 10^{-2}$	$1.30 \cdot 10^{-2}$	$6.78 \cdot 10^{-1}$	$2.78 \cdot 10^{-1}$	1.53	1.03	42.8
12	1.80	$7.04 \cdot 10^{-2}$	$1.30 \cdot 10^{-2}$	$6.78 \cdot 10^{-1}$	$2.77 \cdot 10^{-1}$	1.53	1.03	42.6
16	1.79	$6.93 \cdot 10^{-2}$	$1.27 \cdot 10^{-2}$	$6.79 \cdot 10^{-1}$	$2.71 \cdot 10^{-1}$	1.52	1.01	41.3
20	1.71	$6.32 \cdot 10^{-2}$	$1.15 \cdot 10^{-2}$	$6.85 \cdot 10^{-1}$	$2.37 \cdot 10^{-1}$	1.47	0.93	35.0
24	1.40	$3.65 \cdot 10^{-2}$	$6.41 \cdot 10^{-3}$	$7.12 \cdot 10^{-1}$	$1.15 \cdot 10^{-1}$	1.28	0.56	14.9
28	1.26	$2.18 \cdot 10^{-2}$	$3.76 \cdot 10^{-3}$	$7.27 \cdot 10^{-1}$	$6.29 \cdot 10^{-2}$	1.20	0.34	7.57
32	1.23	$1.87 \cdot 10^{-2}$	$3.20 \cdot 10^{-3}$	$7.30 \cdot 10^{-1}$	$5.29 \cdot 10^{-2}$	1.18	0.29	6.27
36	1.22	$1.74 \cdot 10^{-2}$	$2.97 \cdot 10^{-3}$	$7.31 \cdot 10^{-1}$	$4.86 \cdot 10^{-2}$	1.17	0.27	5.73
40	1.22	$1.77 \cdot 10^{-2}$	$3.02 \cdot 10^{-3}$	$7.31 \cdot 10^{-1}$	$4.96 \cdot 10^{-2}$	1.17	0.28	5.85
44	1.22	$1.79 \cdot 10^{-2}$	$3.06 \cdot 10^{-3}$	$7.31 \cdot 10^{-1}$	$5.02 \cdot 10^{-2}$	1.17	0.28	5.93
48	1.22	$1.68 \cdot 10^{-2}$	$2.87 \cdot 10^{-3}$	$7.32 \cdot 10^{-1}$	$4.69 \cdot 10^{-2}$	1.17	0.27	5.52
52	1.21	$1.66 \cdot 10^{-2}$	$2.84 \cdot 10^{-3}$	$7.32 \cdot 10^{-1}$	$4.64 \cdot 10^{-2}$	1.17	0.26	5.44
56	1.21	$1.65 \cdot 10^{-2}$	$2.81 \cdot 10^{-3}$	$7.32 \cdot 10^{-1}$	$4.59 \cdot 10^{-2}$	1.17	0.26	5.39
60	1.21	$1.67 \cdot 10^{-2}$	$2.85 \cdot 10^{-3}$	$7.32 \cdot 10^{-1}$	$4.66 \cdot 10^{-2}$	1.17	0.26	5.48
64	1.21	$1.63 \cdot 10^{-2}$	$2.79 \cdot 10^{-3}$	$7.32 \cdot 10^{-1}$	$4.55 \cdot 10^{-2}$	1.17	0.26	5.34
68	1.21	$1.66 \cdot 10^{-2}$	$2.84 \cdot 10^{-3}$	$7.32 \cdot 10^{-1}$	$4.64 \cdot 10^{-2}$	1.17	0.26	5.44
72	1.21	$1.67 \cdot 10^{-2}$	$2.85 \cdot 10^{-3}$	$7.32 \cdot 10^{-1}$	$4.66 \cdot 10^{-2}$	1.17	0.26	5.48

concentration, and thus, free calcium concentration was neglected in the model and Eq. (5), can be rewritten as:

$$t_{Ca^{2+}} = [Ca^{2+}] + [CaLac^+] + [CaGlu^+] \approx [CaLac^+] + [CaGlu^+] \quad (8)$$

At time t = 0, it assumed that total calcium concentration is equal to total calcium L-lactate complex concentration, $t_{Ca^{2+}} = [CaLac^+]$, and that calcium D-gluconate is formed as t > 0. Thus, the reaction scheme is given as:

$$CaLac^+ + Glu^- \rightarrow CaGlu^+ + Lac^-,\ k_1 \quad (9)$$

$$CaGlu^+ + Lac^- \rightarrow CaLac^+ + Glu^-,\ k_2 \quad (10)$$

$$CaGlu^+ + Glu^- \rightarrow CaGlu_2(s) \quad (11)$$

$$CaGlu_2(s) \rightarrow CaGlu^+ + Glu^- \quad (12)$$

A steady-state approximation was assumed for D-gluconate concentration, since its concentration is between 3.4 and 5.2 times larger than total calcium concentration. By the law of mass action, calcium L-lactate rate of change is given as:

$$\frac{d}{dt}[CaLac^+] = -k[CaLac^+] + k_2[CaGlu^+][Lac^-] \quad (13)$$

where $k = k_1[Glu^-]$ is a pseudo first order reaction rate constant. Considering that total L-lactate concentration is given by $t_{Lac^-} = [Lac^-] + [CaLac^+]$ and that the equilibrium constant, $K = k_1/k_2$, Eq. (13) can be rewritten as:

$$\frac{d}{dt}[CaLac^+] = -k\left(1 + \frac{[CaGlu^+]}{K[Glu^-]}\right)[CaLac^+] + \frac{kt_{Lac^-}}{K[Glu^-]}[CaGlu^+] \quad (14)$$

where the equilibrium constant K is given by $K = K_2/K_1 = 1.75$, where K_1 and K_2 are given by Eqs. (2) and (4), respectively. Notably in this treatment, a chemical equilibrium is not assumed rather a steady state. The total L-lactate concentration is given by $t_{Lac^-} = 2n_{CaLac_2}/V$, where $2n_{CaLac_2} = 0.014$mol, from the mass of calcium L-lactate, and $[Glu^-] = 1.85$, 2.48, and 2.14 mol L^{-1} for samples A, B and C_d, respectively. Likewise, for calcium D-gluconate:

$$\frac{d}{dt}[CaGlu^+] = k\left(1 + \frac{[CaGlu^+]}{K[Glu^-]}\right)[CaLac^+] - \frac{kt_{Lac^-}}{K[Glu^-]}[CaGlu^+] - r_p + r_d \quad (15)$$

where r_p and r_d are the precipitation and dissolution rates of calcium D-gluconate, respectively. For the precipitation of calcium D-gluconate, it was assumed that $r_p \propto A[Glu^-][CaGlu^+]$, where A corresponds to the total crystalline surface area of calcium D-gluconate. Since D-gluconate ion concentrations was considered to be constant, the rate of

Table 3
Ion speciation for sample B, concentrations expressed in mol L^{-1} and time expressed in hours. Total L-lactate concentration, t_{Lac^-}, equal to $6.71 \cdot 10^{-1}$ mol L^{-1}.

Time	t_{Glu^-}	$[CaLac^+]$	$[Ca^{2+}]$	$[Lac^-]$	$[CaGlu^+]$	$[Glu^-]$	Q_L/K_{sp_L}	Q_G/K_{sp_G}
0.02	2.47	$4.87 \cdot 10^{-2}$	$9.78 \cdot 10^{-3}$	$6.22 \cdot 10^{-1}$	$2.97 \cdot 10^{-1}$	2.17	0.65	64.8
4	2.44	$4.72 \cdot 10^{-2}$	$9.46 \cdot 10^{-3}$	$6.24 \cdot 10^{-1}$	$2.85 \cdot 10^{-1}$	2.15	0.64	61.8
8	2.45	$4.75 \cdot 10^{-2}$	$9.53 \cdot 10^{-3}$	$6.24 \cdot 10^{-1}$	$2.88 \cdot 10^{-1}$	2.16	0.64	62.4
12	2.29	$3.87 \cdot 10^{-2}$	$7.65 \cdot 10^{-3}$	$6.32 \cdot 10^{-1}$	$2.22 \cdot 10^{-1}$	2.07	0.53	46.2
16	2.06	$2.34 \cdot 10^{-2}$	$4.52 \cdot 10^{-3}$	$6.48 \cdot 10^{-1}$	$1.22 \cdot 10^{-1}$	1.93	0.33	23.8
20	1.92	$1.34 \cdot 10^{-2}$	$2.55 \cdot 10^{-3}$	$6.58 \cdot 10^{-1}$	$6.63 \cdot 10^{-2}$	1.85	0.19	12.4
24	1.88	$1.05 \cdot 10^{-2}$	$1.99 \cdot 10^{-3}$	$6.61 \cdot 10^{-1}$	$5.10 \cdot 10^{-2}$	1.83	0.15	9.40
28	1.87	$9.87 \cdot 10^{-3}$	$1.87 \cdot 10^{-3}$	$6.61 \cdot 10^{-1}$	$4.77 \cdot 10^{-2}$	1.83	0.14	8.77
32	1.88	$1.04 \cdot 10^{-2}$	$1.96 \cdot 10^{-3}$	$6.61 \cdot 10^{-1}$	$5.02 \cdot 10^{-2}$	1.83	0.15	9.24
36	1.87	$9.43 \cdot 10^{-3}$	$1.78 \cdot 10^{-3}$	$6.62 \cdot 10^{-1}$	$4.55 \cdot 10^{-2}$	1.82	0.13	8.34
40	1.86	$9.96 \cdot 10^{-3}$	$1.88 \cdot 10^{-3}$	$6.61 \cdot 10^{-1}$	$4.82 \cdot 10^{-2}$	1.83	0.14	8.86
44	1.87	$9.72 \cdot 10^{-3}$	$1.84 \cdot 10^{-3}$	$6.61 \cdot 10^{-1}$	$4.70 \cdot 10^{-2}$	1.83	0.14	8.62
48	1.86	$9.09 \cdot 10^{-3}$	$1.72 \cdot 10^{-3}$	$6.62 \cdot 10^{-1}$	$4.37 \cdot 10^{-2}$	1.82	0.13	8.01
52	1.87	$9.18 \cdot 10^{-3}$	$1.73 \cdot 10^{-3}$	$6.62 \cdot 10^{-1}$	$4.42 \cdot 10^{-2}$	1.82	0.13	8.10
56	1.87	$9.44 \cdot 10^{-3}$	$1.78 \cdot 10^{-3}$	$6.62 \cdot 10^{-1}$	$4.55 \cdot 10^{-2}$	1.82	0.13	8.35
60	1.87	$9.35 \cdot 10^{-3}$	$1.77 \cdot 10^{-3}$	$6.62 \cdot 10^{-1}$	$4.51 \cdot 10^{-2}$	1.82	0.13	8.26
64	1.87	$9.23 \cdot 10^{-3}$	$1.74 \cdot 10^{-3}$	$6.62 \cdot 10^{-1}$	$4.45 \cdot 10^{-2}$	1.82	0.13	8.15
68	1.87	$9.38 \cdot 10^{-3}$	$1.77 \cdot 10^{-3}$	$6.62 \cdot 10^{-1}$	$4.52 \cdot 10^{-2}$	1.82	0.13	8.30
72	1.86	$8.92 \cdot 10^{-3}$	$1.68 \cdot 10^{-3}$	$6.62 \cdot 10^{-1}$	$4.29 \cdot 10^{-2}$	1.82	0.13	7.85

Table 4
Ion speciation for sample C, concentrations expressed in mol L^{-1} and time expressed in hours. Total L-lactate concentration, t_{Lac^-}, equal to $6.95 \cdot 10^{-1}$ mol L^{-1}.

Time	t_{Glu^-}	$[CaLac^+]$	$[Ca^{2+}]$	$[Lac^-]$	$[CaGlu^+]$	$[Glu^-]$	Q_L/K_{sp_L}	Q_G/K_{sp_G}
0.02	2.13	$5.90 \cdot 10^{-2}$	$1.16 \cdot 10^{-2}$	$6.36 \cdot 10^{-1}$	$2.97 \cdot 10^{-1}$	1.83	0.81	54.8
4	2.08	$5.61 \cdot 10^{-2}$	$1.10 \cdot 10^{-2}$	$6.39 \cdot 10^{-1}$	$2.77 \cdot 10^{-1}$	1.80	0.77	50.3
8	2.06	$5.46 \cdot 10^{-2}$	$1.07 \cdot 10^{-2}$	$6.40 \cdot 10^{-1}$	$2.67 \cdot 10^{-1}$	1.79	0.75	48.1
12	2.06	$5.47 \cdot 10^{-2}$	$1.07 \cdot 10^{-2}$	$6.40 \cdot 10^{-1}$	$2.67 \cdot 10^{-1}$	1.79	0.75	48.2
16	2.06	$5.50 \cdot 10^{-2}$	$1.07 \cdot 10^{-2}$	$6.40 \cdot 10^{-1}$	$2.70 \cdot 10^{-1}$	1.79	0.76	48.7
20	2.04	$5.34 \cdot 10^{-2}$	$1.04 \cdot 10^{-2}$	$6.41 \cdot 10^{-1}$	$2.59 \cdot 10^{-1}$	1.78	0.74	46.4
24	2.01	$5.16 \cdot 10^{-2}$	$1.00 \cdot 10^{-2}$	$6.43 \cdot 10^{-1}$	$2.48 \cdot 10^{-1}$	1.76	0.72	43.9
28	1.99	$5.04 \cdot 10^{-2}$	$9.78 \cdot 10^{-3}$	$6.45 \cdot 10^{-1}$	$2.40 \cdot 10^{-1}$	1.75	0.70	42.3
32	1.90	$4.42 \cdot 10^{-2}$	$8.50 \cdot 10^{-3}$	$6.51 \cdot 10^{-1}$	$2.02 \cdot 10^{-1}$	1.70	0.62	34.6
36	1.80	$3.67 \cdot 10^{-2}$	$6.96 \cdot 10^{-3}$	$6.58 \cdot 10^{-1}$	$1.60 \cdot 10^{-1}$	1.64	0.52	26.3
40	1.66	$2.50 \cdot 10^{-2}$	$4.66 \cdot 10^{-3}$	$6.70 \cdot 10^{-1}$	$1.01 \cdot 10^{-1}$	1.55	0.36	15.9
44	1.63	$2.30 \cdot 10^{-2}$	$4.28 \cdot 10^{-3}$	$6.72 \cdot 10^{-1}$	$9.22 \cdot 10^{-2}$	1.54	0.33	14.3
48	1.52	$1.24 \cdot 10^{-2}$	$2.28 \cdot 10^{-3}$	$6.83 \cdot 10^{-1}$	$4.68 \cdot 10^{-2}$	1.47	0.18	6.92
52	1.51	$1.18 \cdot 10^{-2}$	$2.16 \cdot 10^{-3}$	$6.83 \cdot 10^{-1}$	$4.42 \cdot 10^{-2}$	1.46	0.17	6.52
56	1.51	$1.17 \cdot 10^{-2}$	$2.15 \cdot 10^{-3}$	$6.83 \cdot 10^{-1}$	$4.40 \cdot 10^{-2}$	1.46	0.17	6.48
60	1.50	$1.14 \cdot 10^{-2}$	$2.08 \cdot 10^{-3}$	$6.84 \cdot 10^{-1}$	$4.25 \cdot 10^{-2}$	1.46	0.17	6.25
64	1.50	$1.11 \cdot 10^{-2}$	$2.03 \cdot 10^{-3}$	$6.84 \cdot 10^{-1}$	$4.14 \cdot 10^{-2}$	1.46	0.16	6.08
68	1.50	$1.09 \cdot 10^{-2}$	$1.99 \cdot 10^{-3}$	$6.84 \cdot 10^{-1}$	$4.07 \cdot 10^{-2}$	1.46	0.16	5.97
72	1.50	$1.10 \cdot 10^{-2}$	$2.01 \cdot 10^{-3}$	$6.84 \cdot 10^{-1}$	$4.10 \cdot 10^{-2}$	1.46	0.16	6.01

precipitation is given by:

$$r_p = k_p A [CaGlu^+] \tag{16}$$

The crystallization starts after a critical nucleation time, t_c, when the calcium D-gluconate crystals form. For spherical crystals, the surface area can be written in terms of the crystal mass of calcium D-gluconate, according to $A \propto r^2 \propto m^{2/3}$, where r is the radius of the crystal. Thus, applying mass conservation of calcium, the precipitation rate is given by:

$$\begin{aligned} r_p &= \alpha [CaGlu^+] m^{2/3} \\ &= \alpha_p [CaGlu^+]([CaLac^+]_0 - [CaLac^+] - [CaGlu^+])^{2/3} \end{aligned} \tag{17}$$

The parameter α_p refers to the precipitation rate parameter, which includes the crystal geometric correction factor and the rate constant k_p. Likewise, for the dissolution rate, it is assumed that $r_d \propto A$, consequently:

$$r_d = k_d A = \alpha_d ([CaLac^+]_0 - [CaLac^+] - [CaGlu^+])^{2/3} \tag{18}$$

where α_d corresponds to the dissolution rate parameter. It is important to mention that $r_d = r_p$ at equilibrium and, therefore, there is a relation between the precipitation and dissolution parameters:

$$\frac{\alpha_d}{\alpha_p} = [CaGlu^+]_{eq} \tag{19}$$

However, the equilibrium concentration of calcium D-gluconate is unknown a priori.

Eqs. (14), (15), (17) and (18) form a non-linear differential system, solved by standard numerical methods (Eaton, Bateman, Hauberg, & Rik, 2020). At time $t \geq t_c$ the precipitation is initiated using a small critical crystal surface A_0.

The model has four parameters, namely, k, α_p, α_d and t_c. which can be determined by fitting the numerical solution to the data. The model output at time was defined as $y = (t, \theta)$, where y is the total calcium concentration, $y = [CaLac^+] + [CaGlu^+]$, and θ is the parameter vector, $\theta = (k, \alpha_p, \alpha_d, t_c)$. In the fitting procedure, the parameter vector is found using minimized cost function, χ^2-function:

$$c(\theta) = \sum_i (t_{Ca^{2+},i} - y(t_i, \theta))^2 \tag{20}$$

where $i > 0$ runs over the number of data points and $t_{Ca^{2+}}$is the experimental data for total calcium concentration. The cost function was minimized with an appropriate initial guess and the Nelder-Mead simplex algorithm (Nelder & Mead, 1965).

Two different fitting protocols were studied. In the first protocol (P-I), the model was fitted for single data series of samples A, B and C_d. In the second protocol (P-II), the parameters were the average values from fitting the model to both samples A and B. Critical nucleation time, t_c, is dependent on the concentration of D-gluconate and, therefore, was fitted independently for all cases giving 17 h, 8 h and 22 h for samples A, B and C_d, respectively. The parameters are listed in Table 5 as results of both protocols and Fig. 2 exhibits both models for samples A, B and C_d.

In the model it is assumed that calcium L-lactate and calcium D-gluconate reach equilibrium distribution before nucleation process begins and that the observed total calcium concentration decay is due to the nucleation process. Since the exact rate at which the system relaxes to equilibrium cannot be determined based on the data, the lower limit of k, k_{min}, was is estimated. This rate constant is a first order rate constant and the overall equilibration process can be characterized as a pseudo first order reaction.

To verify the dependency of α_p and α_d and how the cost function c depends on these two parameters, a contour plot of c, with fixed k and t_c values from protocol P-I, was performed and is exhibited in Fig. 3.

From the characteristic contour (Gutenkunst et al., 2007), it is possible to verify the ellipses major axis (sloppy direction) in which the cost function is not greatly affected with simultaneous variation of α_p and α_d, and the ellipses minor axis (stiff direction) in which the cost function increases abruptly as α_p and α_d vary. The different directions are parallel to eigenvector of the Hessian 2×2 matrix $H_{ij} = \partial^2 c / \partial \alpha_i \partial \alpha_j$, in which indices i and j take values p and d. The ratio of the eigenvalues was found to be around 25, therefore the model allows for a rather sloppy parameter combination with respect to the precipitation and dissolution rate parameters.

The Metropolis Monte-Carlo method (Frederiksen, Jacobsen, Brown, & Sethna, 2004) was applied to quantify the statistical uncertainty of the model output. In the Monte-Carlos method the parameters vary iteratively as $\theta_{i+1} = \theta_i + \delta\theta$, where $\delta\theta$ is a small incremental vector with vector elements that are uniformly distributed

Table 5
Fitted model parameter values using the two different protocols P-I and P-PII.

Parameter		Water		Deuterium oxide
		P-I	P-II	P-I
k_{min}	h^{-1}	0.20	0.20	0.15
α_d	$h^{-1}\ M^{1/3}$	0.08	0.07	0.02
α_p	$h^{-1}\ M^{2/3}$	1.63	1.45	0.72

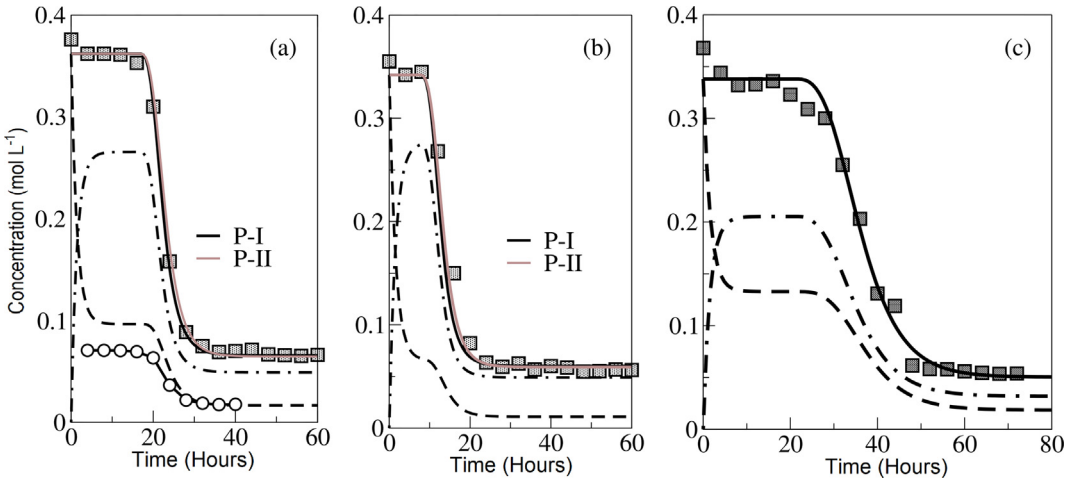

Fig. 2. (a) Model fit to sample A, (b) model fit to sample B and (c) model fit to sample C_d. Full black line represents total calcium concentration from fitting protocol P-I. Full red line represents total calcium concentration from fitting protocol P-II. The dashed line represents calcium L-lactate complex concentration and the dot-dashed line represents calcium D-gluconate complex concentration. In (a) the calculated calcium L-lactate complex concentration, Table 2, is also shown for comparison as (circles connected with lines).

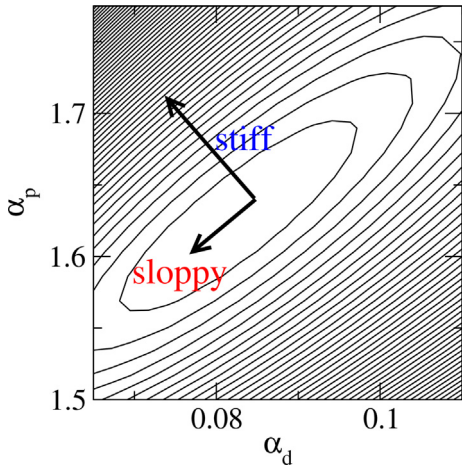

Fig. 3. Contour plot of the cost function, c, for sample A. k = 0.21 h^{-1} and t_0 = 17.1 h, in accordance with protocol P-1.

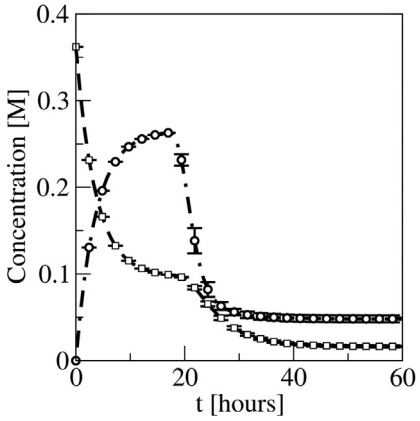

Fig. 4. Statistical uncertainty of the model output for Sample A. The dashed line represents calcium L-lactate complex concentration and the dot-dashed line represents calcium D-gluconate complex concentration. The errorbars represent the standard deviation of the model output when using the Monte-Carlos parameter set.

random number with zero mean. If $c(\theta_{i+1}) \geq c(\theta_i)$ the new parameter set is only accepted if $\chi < e^{c(\theta_{i+1})/c(\theta_i)-1}$ where χ is a random number from a uniform distribution in the interval from 0 to 1. The parameter output from the best fit is used as the initial parameter set θ_1 and then 10^5 parameter sets is generated. The maximum value for the incremental vector is set such that approximately half of the iterations lead to an accepting iteration. In order to reduce spurious correlations, only every ten accepted parameter set is stored, giving 10^4 sets for further analysis. The model is integrated for the stored parameter set and the output is shown in Fig. 4 for sample A. Clearly the model output features vary little variation with the parameters.

In aqueous solutions calcium is known to exchange ligands in fast reactions, at least under natural and acidic conditions (Carr & Swartzfager, 1975; Cvetković, Jovanović, Maćešić, & Adnađević, 2018; Gao et al., 2010; Zhou, Xue, & Yang, 2013). For partially digested foods, the pH change upon transfer of the chyme from the stomach to the intestines where calcium is absorbed, and the high viscosity may slow down the calcium ligand exchange reactions. Still such reactions seem fast with half-lives of only a few minutes, as has been found for water/ethanol exchange in calcium hydrogels (Cvetković et al., 2018). Hydration of calcium is strongly dependent on the presence of simple salts such as alkali halides, which determines the hydrogen bonding network and ligand exchange around calcium ions, further affecting the mobility of the calcium ions (Di Tommaso, Ruiz-Agudo, De Leeuw, Putnis, & Putnis, 2014). These aspects need both to be considered for a more quantitative description of the bioavailability of calcium.

The deuterium/hydrogen isotope effect of 1.25 could indicate an involvement of hydrogen bonding in the dissociation of a hydroxycarboxylate from the primary coordination sphere of calcium prior to coordination of the incoming hydroxycarboxylate pointing towards ligand dissociation and change in coordination number as rate determining.

The well-established effects of hydroxycarboxylates like L-lactate, D-gluconate, D-lactobionate and citrate on increasing calcium bioavailability may relate to longer half-life for exchange of hydroxycarboxylates as ligands coordinated to calcium. However, a change in calcium mobility in aqueous solution with high concentrations of ligands involved in hydrogen bonding with water molecules may also affect calcium hydration and further phase transitions, including precipitation.

The unique phenomenon of spontaneous non-thermal supersaturation of calcium hydroxycarboxylates has now, through our modelling based on numerical solution of coupled differential

equations, found an explanation. The exchange between L-lactate and D-gluconate coordinated to calcium becomes slow with half-life of 5 h, probably due to a combination of an increasing viscosity and a change in hydrogen bonding with water molecules. Previous studies have shown that the rate of precipitation for supersaturated calcium D-gluconate solutions depends on a reaction between a calcium D-gluconate complex ion and a free D-gluconate ion, as described in Eq. (11). The rate of this reaction will be slower for conditions where the exchange equilibration is slow, as in the reaction of Eq. (9).

4. Conclusions

The kinetic characterization of the precipitation of calcium D-gluconate from the spontaneously supersaturated calcium L-lactate/D-gluconate solutions have helped to understand surprising high supersaturation occurring spontaneously without heating and the robustness of calcium hydroxycarboxylate supersaturation. The slow ligand exchange in the hydroxycarboxylate complexes of calcium slows down the formation of ions actively involved in the precipitation reaction. Such slow exchange reactions now demonstrated for L-lactate/D-gluconate may be of more general importance for biomineralization and this also explain the superiority of calcium hydroxycarboxylates as calcium supplement as they will stay supersaturated in the intestines facilitating calcium paracellular absorption. Further studies will be required for an explanation of the beneficial effect of a high citrate circulation on mineralization and high bone strength.

CRediT authorship contribution statement

André C. Garcia: Conceptualization, Methodology, Investigation. **Jesper S. Hansen:** Methodology, Software. **Nicholas Bailey:** Methodology, Software. **Leif H. Skibsted:** Conceptualization, Methodology.

Declaration of Competing Interest

The authors declare that they have no known competing financial interests or personal relationships that could have appeared to influence the work reported in this paper.

Acknowledgments

The Danish Dairy Research Foundation and Arla Foods Ingredients are thanked for supporting the project. This study was also financed by a grant from Coordenação de Aperfeiçoamento Pessoal de Nível Superior (CAPES) to André C. Garcia (Process 12963/13-5 CAPES/Science Without Borders).

References

Adluri, R. S., Zhan, L., Bagchi, M., Maulik, N., & Maulik, G. (2010). Comparative effects of a novel plant-based calcium supplement with two common calcium salts on proliferation and mineralization in human osteoblast cells. *Molecular and Cellular Biochemistry, 340*(1–2), 73–80.

de Barboza, G. D., Guizzardi, S., & de Talamoni, N. T. (2015). Molecular aspects of intestinal calcium absorption. *World Journal of Gastroenterology, 21*(23), 7142–7154.

Carr, J. D., & Swartzfager, D. G. (1975). Kinetics of the ligand exchange and dissociation reactions of calcium-aminocarboxylate complexes. *Journal of the American Chemical Society, 97*(2), 315–321.

Cvetković, N. M., Jovanović, J. D., Maćešić, S. R., & Adnađević, B. K. (2018). Isothermal kinetics of exchange of water absorbed in calcium alginate hydrogel with ethanol. *Chemical Industry and Chemical Engineering Quarterly, 24*(3), 275–281.

de Boland, A. R., Garner, G. B., & O'Dell, B. L. (1975). Identification and properties of "phytate" in cereal grains and oilseed products. *Journal of Agricultural and Food Chemistry, 23*(6), 1186–1189.

Di Tommaso, D., Ruiz-Agudo, E., De Leeuw, N. H., Putnis, A., & Putnis, C. V. (2014). Modelling the effects of salt solutions on the hydration of calcium ions. *Physical Chemistry Chemical Physics, 16*(17), 7772–7785.

Eaton, J. W., Bateman, D., Hauberg, S., & Rik, W. (2020). GNU Octave: A high-level interactive language for numerical computations. Version 5.2.0.

Frederiksen, S. L., Jacobsen, K. W., Brown, K. S., & Sethna, J. P. (2004). Bayesian ensemble approach to error estimation of interatomic potentials. *Physical Review Letters, 93*(16), 1–4.

Gao, R., van Halsema, F. E. D., Temminghoff, E. J. M., van Leeuwen, H. P., van Valenberg, H. J. F., Eisner, M. D., … van Boekel, M. A. J. S. (2010). Modelling ion composition in simulated milk ultrafiltrate (SMUF). I: Influence of calcium phosphate precipitation. *Food Chemistry, 122*(3), 700–709.

Garcia, A. C., Vavrusova, M., & Skibsted, L. H. (2016). Calcium d-saccharate: Aqueous solubility, complex formation, and stabilization of supersaturation. *Journal of Agricultural and Food Chemistry, 64*(11), 2352–2360.

Garcia, A. C., Vavrusova, M., & Skibsted, L. H. (2018). Supersaturation of calcium citrate as a mechanism behind enhanced availability of calcium phosphates by presence of citrate. *Food Research International, 107*(February), 195–205.

Gutenkunst, R. N., Waterfall, J. J., Casey, F. P., Brown, K. S., Myers, C. R., & Sethna, J. P. (2007). Universally sloppy parameter sensitivities in systems biology models. *PLoS Computational Biology, 3*(10), 1871–1878.

Hartley, A., Paternoster, L., Evans, D., Fraser, W., Tang, J., Lawlor, D., … Gregson, C. (2019). Metabolomics analysis in adults with high bone mass identifies a relationship between bone resorption and circulating citrate which replicates in the general population. *Clinical Endocrinology, 92*, 29–37.

Holt, C., Lenton, S., Nylander, T., Sørensen, E. S., & Teixeira, S. C. M. (2014). Mineralisation of soft and hard tissues and the stability of biofluids. *Journal of Structural Biology, 185*(3), 383–396.

Nelder, J. A., & Mead, R. (1965). A simplex method for function minimization. *The Computer Journal, 7*(4), 308–313.

Pak, C. Y. C., Harvey, J. A., & Hsu, M. C. (1987). Enhanced calcium bioavailability from a solubilized form of calcium citrate. *Journal of Clinical Endocrinology and Metabolism, 65*(4), 801–805.

Siegrist, V. H. (1949). Kalziumglukonat-Injektionslösungen mit Zusatz von Kalziumlaevulinat bzw. Kalzium-d-saccharat. *Pharmaceutica Acta Helvetiae,* 12.

Tondapu, P., Provost, D., Adams-Huet, B., Sims, T., Chang, C., & Sakhaee, K. (2009). Comparison of the absorption of calcium carbonate and calcium citrate after roux-en-Y gastric bypass. *Obesity Surgery, 19*(9), 1256–1261.

Vavrusova, M., Danielsen, B. P., Garcia, A. C., & Skibsted, L. H. (2018). Codissolution of calcium hydrogenphosphate and sodium hydrogencitrate in water. Spontaneous supersaturation of calcium citrate increasing calcium bioavailability. *Journal of Food and Drug Analysis, 26*(1), 330–336.

Vavrusova, M., Garcia, A. C., Danielsen, B. P., & Skibsted, L. H. (2017). Spontaneous supersaturation of calcium citrate from simultaneous isothermal dissolution of sodium citrate and sparingly soluble calcium hydroxycarboxylates in water. *RSC Advances, 7*(6), 3078–3088.

Vavrusova, M., Liang, R., & Skibsted, L. H. (2014). Thermodynamics of dissolution of calcium hydroxycarboxylates in water. *Journal of Agricultural and Food Chemistry, 62*(24), 5675–5681.

Vavrusova, M., Munk, M. B., & Skibsted, L. H. (2013). Aqueous solubility of calcium L-lactate, calcium D-gluconate, and calcium D-lactobionate: Importance of complex formation for solubility increase by hydroxycarboxylate mixtures. *Journal of Agricultural and Food Chemistry, 61*(34), 8207–8214.

Vavrusova, M., & Skibsted, L. H. (2014). Spontaneous supersaturation of calcium d-gluconate during isothermal dissolution of calcium l-lactate in aqueous sodium d-gluconate. *Food and Function, 5*(1), 85–91.

Wang, L.-M., Wang, W., Li, X., Peng, L., Lin, Z. Q., & Xü, H. (2012). Calcium citrate: A new biomaterial that can enhance bone formation in situ. *Chinese Journal of Traumatology - English Edition, 15*(5), 291–296.

Wasserman, R. H. (2004). Vitamin D and the dual processes of intestinal calcium absorption. *The Journal of Nutrition, 134*(11), 3137–3139.

Zhou, Y., Xue, S., & Yang, J. J. (2013). Calciomics: Integrative studies of Ca^{2+}-binding proteins and their interactomes in biological systems. *Metallomics, 5*(1), 29–42.